BRLR 1291

BRL

AD

REPORT NO. 1291

AN ATTITUDE DETERMINING SYSTEM FOR SPINNING ROCKETS

by

Joseph M. Conley
R. B. Patton, Jr.

December 1965

U. S. ARMY MATERIEL COMMAND
BALLISTIC RESEARCH LABORATORIES
ABERDEEN PROVING GROUND, MARYLAND

B A L L I S T I C R E S E A R C H L A B O R A T O R I E S

REPORT NO. 1291

DECEMBER 1965

Distribution of this document is unlimited.

AN ATTITUDE DETERMINING SYSTEM FOR SPINNING ROCKETS

Joseph M. Conley
R. B. Patton, Jr.

Ballistic Measurements Laboratory

RDT&E Project No. 1V014501B53A

A B E R D E E N P R O V I N G G R O U N D, M A R Y L A N D

B A L L I S T I C R E S E A R C H L A B O R A T O R I E S

REPORT NO. 1291

JMConley/RBPatton,Jr./blw
Aberdeen Proving Ground, Md.
December 1965

AN ATTITUDE DETERMINING SYSTEM FOR SPINNING ROCKETS

ABSTRACT

An attitude sensor for spinning rockets and the associated digital computing procedure have been developed and tested. The measuring system consists of a commercially available flux gate magnetometer and a single solar cell with a fan-shaped acceptance beam. The computing procedure is designed to improve approximations of the rocket aspect angles by successive differential corrections which are derived by a least squares treatment of an overdetermined system of condition equations.

Both the measuring system and the computing methods have been found to provide a practical approach for determining rocket aspect. The system is estimated to have been accurate to between one and two degrees in its initial test and to have a potential accuracy of better than one degree.

TABLE OF CONTENTS

TABLE OF SYMBOLS

l	direction cosine with respect to X-axis
m	direction cosine with respect to Y-axis
n	direction cosine with respect to Z-axis
t	time of observation
u	normalized value of E, i.e. cos λ
A	matrix for transformation from body to space coordinate system
$\vec{C}$	vector in $X'Y'$-plane from origin through slit in missile skin
D	denominator of Equation (18)
E	observations recorded for the magnetometer in volts
$\vec{H}$	the Earth's magnetic field vector
J	the Jacobian matrix $\left(\frac{u_1, u_2, \ldots, u_k}{\theta, \phi}\right)$
$\vec{M}$	vector in the direction of the axis of the magnetometer
N	the numerator of Equation (18)
R	a rotation matrix
$\vec{S}$	vector from the origin toward the sun
ΔU	a column matrix of the residuals
W	column matrix whose elements are θ and ϕ
ΔW	column matrix whose elements are $\Delta\theta$ and $\Delta\phi$
X	coordinate to the south in the space system
Y	coordinate to the east in the space system
Z	vertical coordinate in the space system
α	azimuth measured counterclockwise from south
γ	angular rotation performed by matrix R
ϵ	elevation angle measured from XY-plane

TABLE OF SYMBOLS (CONTD)

θ	angular rotation about line of nodes OP
λ	angle formed by vectors $\vec{M}$ and $\vec{H}$
ϕ	angular rotation about Z-axis
ψ	angular rotation about Z'-axis
ω	angle between the X'-axis and $\vec{C}$

Subscripts

c	computed value
f	end of reduction interval
i	refers to ith observation in reduction interval
j	specifies rotation axis
k	upper limit of the parameter i
o	beginning of reduction interval
ob	observed value
C	refers to vector $\vec{C}$
H	refers to vector $\vec{H}$
M	refers to vector $\vec{M}$
S	refers to vector $\vec{S}$

Superscripts

'	refers to body coordinate system
$\cdot$	differentiation with respect to time

INTRODUCTION

The purpose of the efforts reported here was to obtain moderately accurate ($\pm 1^{o}$) measurements of sounding rocket attitude with a minimum of construction expense, time, and calibration. Because of the ready availability of a reliable and easily used flux gate magnetometer, a large proportion of sounding rockets incorporate such an instrument for qualitative aspect information, i.e., orientation with respect to the geomagnetic field vector only[1,2*]. Israel, et. al., have reported the determination of complete aspect information from magnetometers only[3]. Solar aspect devices have also been used for qualitative aspect measurements with respect to the rocket-sun vector[4,5]. Schemes involving one or more magnetometers and calibrated or uncalibrated photo-detectors have been reported for acquisition of complete orientation information[6,7]. The system described herein has the advantage that only an uncalibrated solar cell or photomultiplier need be added to the normally present aspect magnetometer in order to obtain complete attitude information for a spinning rocket. The magnetometer is factory calibrated and yields the angle between the rocket axis and the geomagnetic field. The solar cell is collimated to a narrow, fan-shaped beam, and the phase of the solar cell pulse relative to the magnetometer signal is used to complete the attitude determination.

A digital computing method has been developed for the reduction of the flight measurements to rocket aspect. This problem requires the evaluation of a set of three parameters to completely specify the orientation of a rigid body. A convenient set of parameters consists of the Eulerian angles[8], two of which determine the attitude of the body while the third describes the rotation of the body about its symmetry axis. By combining certain simplifying assumptions with the observations recorded for the solar cell, it becomes possible to express the third parameter as a function of the other two Eulerian angles. Hence, the problem reduces to the determination of two angles which vary with time.

---

* *Superscript numbers denote references which may be found on page 47.*

Moreover, these angles completely describe the aspect of the rocket. Since the measured quantities are nonlinear functions of the Eulerian angles, it is convenient to evaluate these angles by a fitting procedure in which a set of approximations is improved by a series of differential corrections. The latter are obtained from a least squares treatment of an overdetermined system of condition equations which are derived from the measurements of the aspect system.

The method of solution was tested on actual field data for a Nike-Apache missile launched at Fort Churchill, Canada. Both the measuring system and the computing procedures were found to provide a practical approach for determining rocket aspect. Generally, the computations converged to the correct solution on the BRLESC computer in approximately 0.6 seconds per point. It is estimated that the aspect system provided an accuracy of better than two degrees in its initial test and further, that its potential accuracy is one degree or better.

INSTRUMENTATION

Figure 1 is a perspective diagram of the magnetometer sensor and solar cell within the rocket payload. The aspect magnetometer was a flux gate instrument capable of about 1 percent accuracy. It was glued to a fiberglass deck plate after being located such that it was normal to the plane containing the optical aperture and the symmetry axis of the rocket. The output of the magnetometer in volts (E) is proportional to the component of the geomagnetic field parallel to the sensor axis. That is,

$$E = 4.0 \, |H| \cos \lambda \, , \qquad (1)$$

where λ is the angle between the geomagnetic field vector $\vec{H}$ (gauss) and the sensor positive axis $\vec{M}$. The solar cell was a commercial unit 5 mm x 5 mm, mounted one inch from a longitudinal aperture in the fiberglass skin of the rocket. The aperture was covered by a fused quartz window to protect the solar cell from aerodynamic effects, but this was probably not necessary.

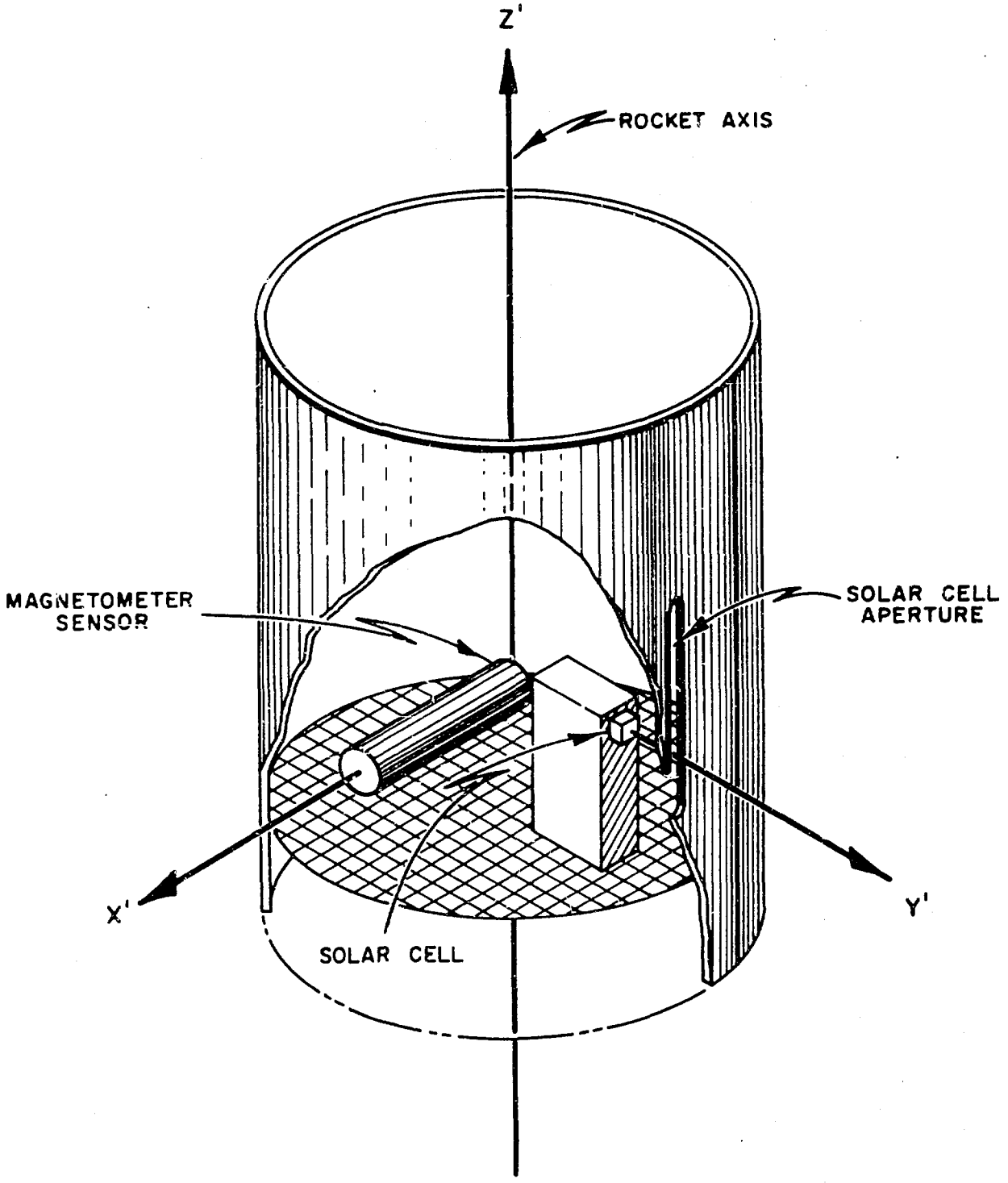

FIG. 1 - ASPECT SYSTEM PERSPECTIVE DIAGRAM

For a rocket with spin frequency much greater than pitch frequency, the transverse aspect magnetometer produces a modulated sinusoidal output signal, the instantaneous amplitude of which defines a cone about the geomagnetic field. As shown in Figure 2, one of the generating elements of this cone coincides with the rocket longitudinal axis. In the aspect system described here a solar cell with a fan-shaped acceptance beam, determined by the slit in the rocket skin, produces a pulse as it sweeps past the sun. Then the phase of this sun pulse relative to the magnetometer signal is a function of the position of the rocket on the previously defined cone. Figure 2 illustrates the relationships between the geomagnetic field, the cone defined by the aspect magnetometer, and the solar cell acceptance beam.

The solar cell and the slit were both 5 mm wide, and the cell was located 25 mm behind the slit. Thus, the angular aperture of the solar cell in the horizontal plane was 23°, but the cell was fully illuminated only instantaneously, at the center of the pulse. This produced an approximately triangular waveform, later differentiated and bandwidth limited. The length of the slit was 3 inches, yielding an angular coverage of $+ 66^{\circ}$ to $- 41^{\circ}$, since the solar cell was not centered vertically. The solid angle coverage was 3.1 π steradians, adequate for the present application. This could be readily extended to 3.8 π steradians with the same slit and two solar cells in parallel, located behind the upper and lower edges of the 3" aperture.

The magnetometer signal was direct coupled into a standard IRIG 10.5 kc subcarrier oscillator (SCO) of an FM/FM telemetry system, as shown in the electrical schematic (Figure 3). The common base amplifier used with the solar cell produces approximately 5 volts signal for solar illumination of normal incidence above the atmosphere. Since the payload construction was nearly complete when the solar cell was added, the sun signal was merely AC coupled into the same SCO used for the magnetometer. The delay of the sun signal relative to the magnetometer signal, at the discriminator output, was approximately 0.3 milliseconds

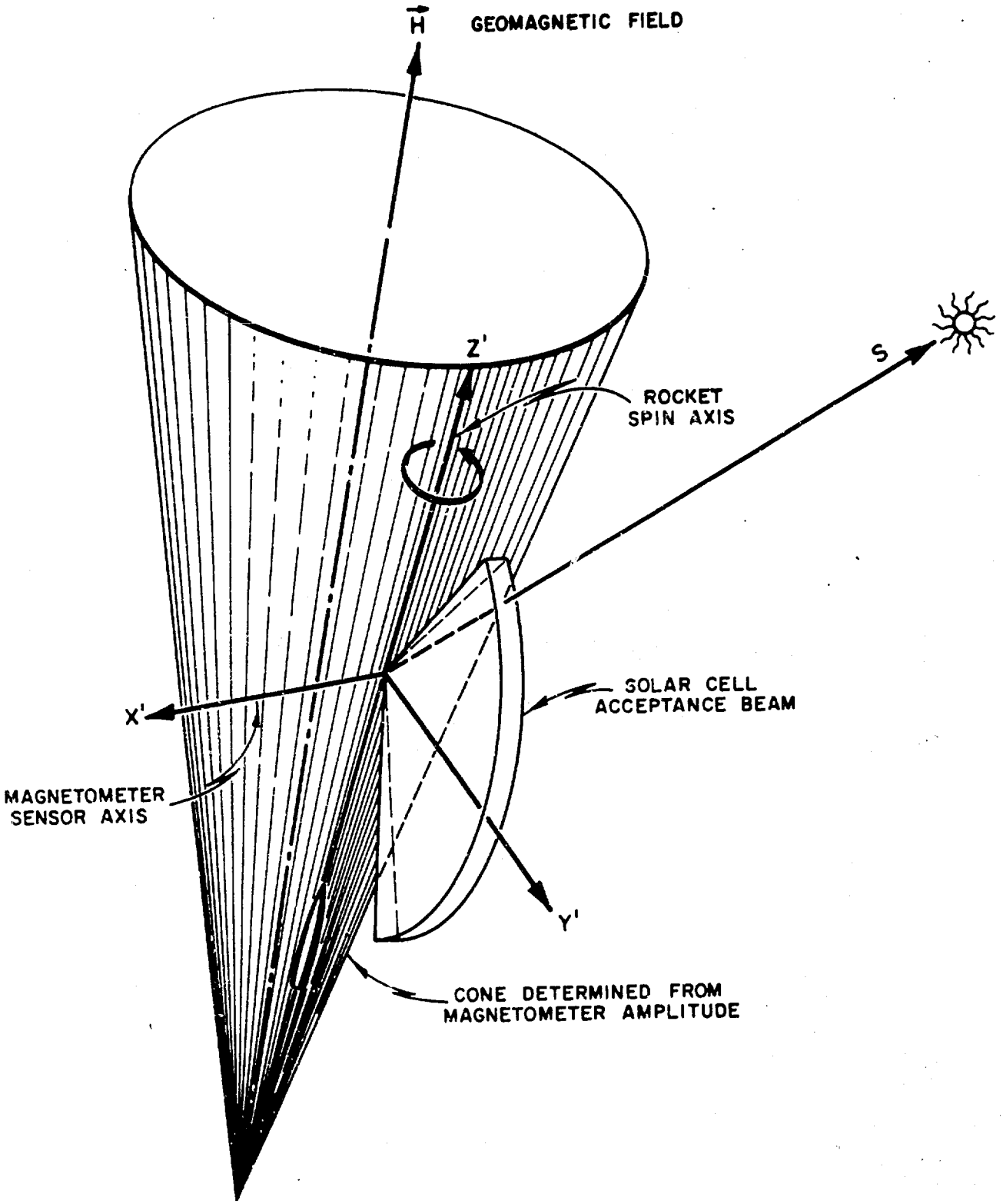

FIG. 2 - SYSTEM GEOMETRY WHILE SOLAR CELL BEAM SWEEPS PAST THE SUN.

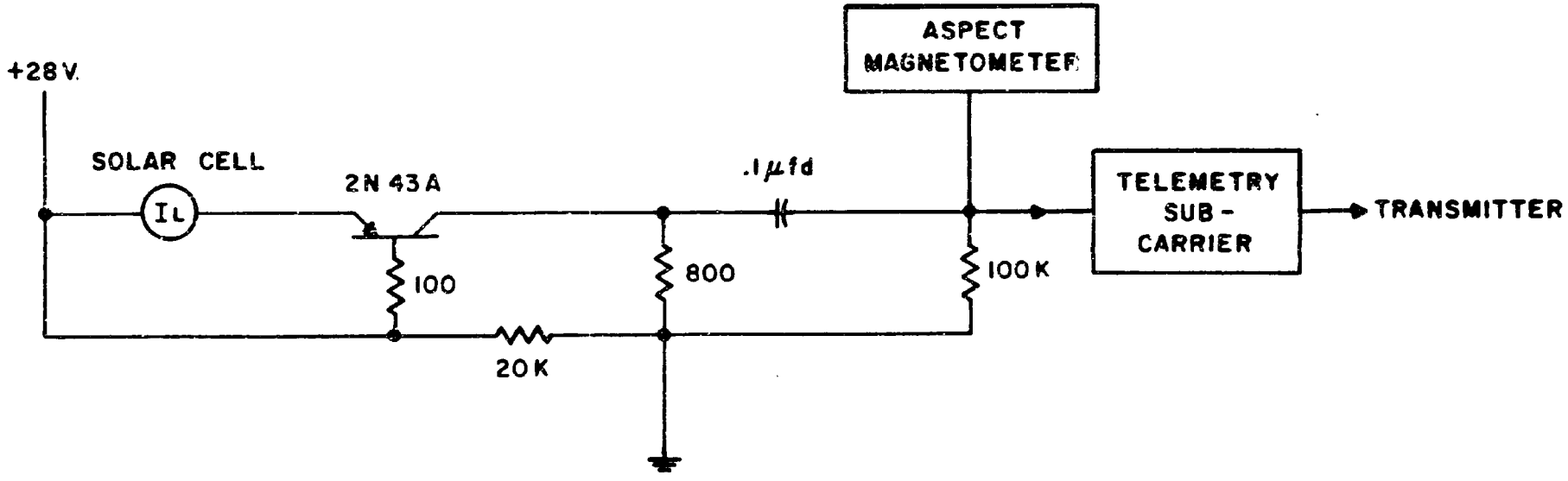

FIGURE 3 - ELECTRICAL SCHEMATIC

for spin rates of 5 to 10 rps, and was considered negligible for this application. For automatic data reduction separate channels for the two functions would be desirable, with appropriate correction for the greater differential delay.

Two typical oscillograms from Nike-Apache rocket No. 14.36 are shown in Figure 4. The slowly varying sinusoidal waveform is the magnetometer output signal, and the transient sun pulse is superimposed on it. The differentiating effect of the AC coupling and the bandwidth limiting of the discriminator filter produced the sun pulse shapes illustrated. The magnetometer signal is essentially undistorted. Sample A is from early in flight while the rocket was nearly vertical. The phase of the sun pulse relative to the magnetometer signal remained nearly constant during this interval. Sample B occurred during rocket turnover upon re-entry into the effective atmosphere. The sun pulse can be seen to shift about 160° in phase during 2.6 seconds of flight time. The sun was outside the solar cell field of view during the first three and the last two of the cycles shown. This particular flight produced poor quality telemetry data. There was complete loss of signal from 37 seconds to 265 seconds and frequent short dropouts occurred from 265 seconds to rocket impact. Even so, the aspect system produced usable data at all times for which the sun signal could be detected.

DEVELOPMENT OF THE COMPUTING PROCEDURE

The method of solution used in reducing the recorded data to missile aspect is predicated upon the assumption of a negligible change in rocket attitude over the time interval of a single revolution of the missile. In fact, for rapidly spinning rockets, we may assume that the aspect remains constant throughout each revolution, but varies from one revolution to another. While this assumption is, perhaps, less valid for slowly spinning missiles, it is still a reasonable approximation for at least the free flight portion of the trajectory. Hence, we consider successive pulses from the solar cell to exactly define the time interval of one complete revolution of the rocket and assume its aspect to remain

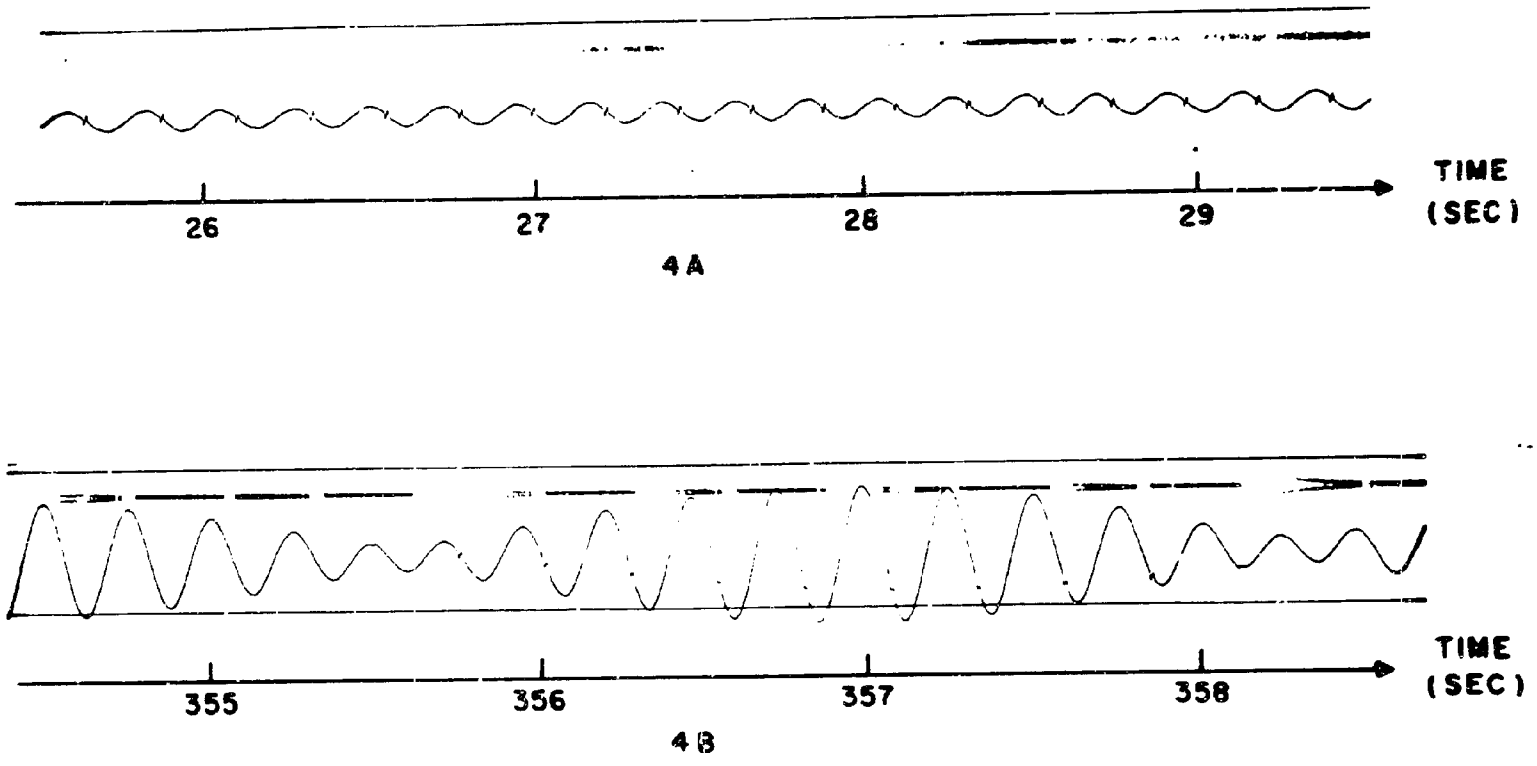

FIGURE 4 – SAMPLE OSCILLOGRAMS FROM NIKE - APACHE 14.36 – ASPECT MAGNETOMETER OUTPUT VOLTAGE VS. ROCKET FLIGHT TIME

constant between pulses. In addition to the solar pulses, only two observations from the magnetometer are required to compute a pair of angles that completely describe the attitude of the missile. Normally, ten to fifteen readings are made between successive pulses to provide considerable overdetermination for the solution. The method of computation consists of a fitting procedure in which a set of approximations for the aspect angles is improved by successive differential corrections. These corrections are obtained from a least squares treatment of the overdetermined system of condition equations that are derived from a Taylor expansion about a point consisting of approximations for the aspect angles. All second and higher order terms of the expansion have been neglected.

The solution will be described for a single revolution of the rocket. The computing method presented here is then merely repeated for each revolution of the missile over its entire trajectory. We define t_o and t_f to be the times of successive solar pulses and hence, based on our assumptions, the initial and final times of one complete revolution of the rocket. The symbol t_i will denote the times of all observations E_i which are recorded for the magnetometer within the interval $[t_o, t_f]$. The subscript i ranges from 1 to k where k is the number of observations in the interval.

In the development of this solution, it is convenient to employ two rectangular coordinate systems, one fixed with respect to the earth and the other fixed with respect to the orientation of the missile body. Referring to Figure 5, the two systems are defined as follows.

1. The XYZ-coordinate system is a right-hand system with the origin on the earth's surface at the launcher. The X-axis is positive south, the Y-axis is positive east, and the Z-axis is normal to the earth's surface at the launching site. This will be referred to as the space coordinate system.

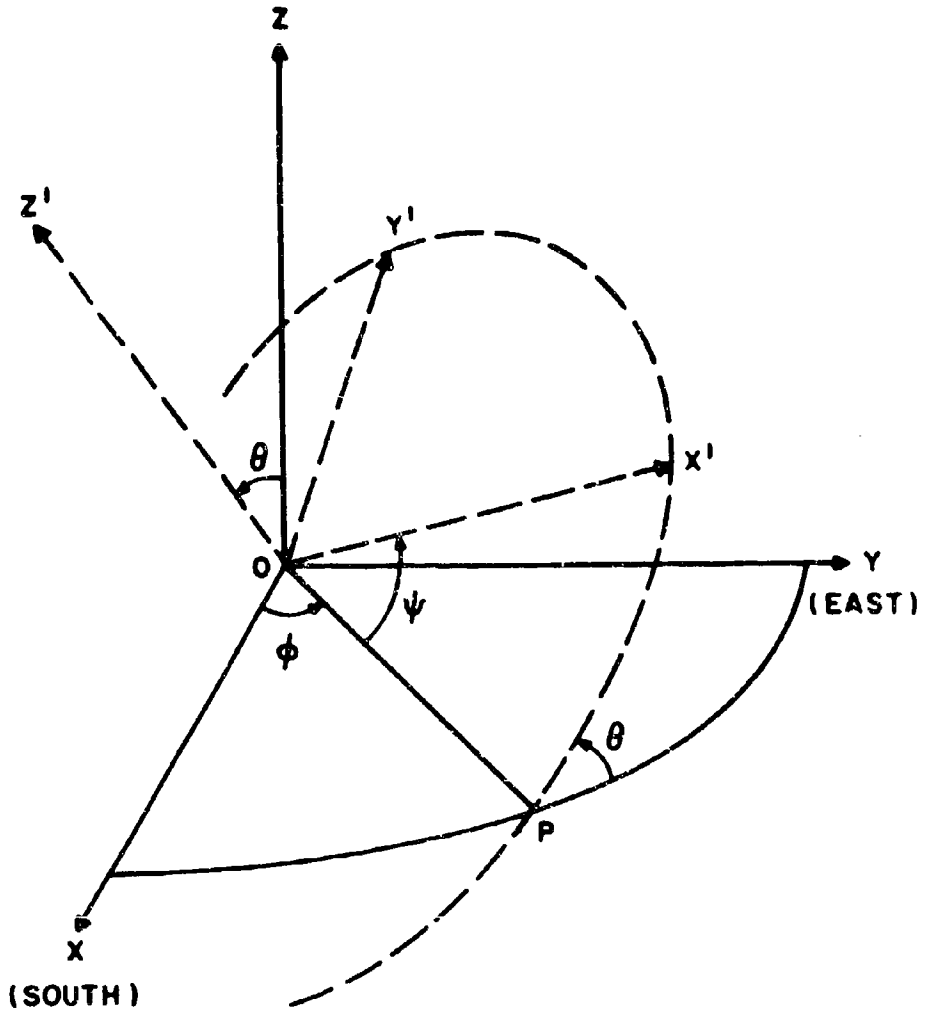

FIGURE 5 - COORDINATE SYSTEM GEOMETRY

2. The X'Y'Z'- coordinate system is a right-hand system with the same origin as the XYZ-system. The Z'-axis is parallel to the symmetry axis of the rocket body while the X'-axis is positive in the direction of the magnetometer axis. The Y'-axis is chosen so as to complete a right-hand system. This will be referred to as the body coordinate system.

In our instrumentation system, the Y'-axis passes through the slit which has been cut in the skin of the rocket for the solar cell. This is a simplifying, but not a necessary, condition for our method of solution. It is convenient to specify the orientation of the body coordinate system with respect to the space system by means of the Eulerian angles ϕ, ψ, and θ as indicated in Figure 5. These angles specify the direction and magnitude of three rotations which, when performed in a specific sequence, will result in a transformation from one of the rectangular coordinate systems to the other. The angles ϕ, θ, and ψ are generated by rotations about the Z-axis, the line of nodes OP, and Z'-axis respectively. All are positive for a right-hand rotation. Let the notation $R_j(\gamma)$ indicate the matrix performing a rotation through an angle γ and the j^{th} axis of the frame of reference, such that the angle is positive for a rotation in the right-hand direction. The symbol j is equal to 1, 2, or 3 according to whether the rotation is about the X, Y, or Z axis, respectively. In this notation, a transformation from the space system to the body system can be accomplished by three rotations as follows: 1) $R_3(\phi)$, 2) $R_1(\theta)$, and 3) $R_3(\psi)$. To transform from the body system to the space system requires the following sequence of rotations: 1) $R_3(-\psi)$, 2) $R_1(-\theta)$, and 3) $R_3(-\phi)$.

On the basis of previous assumptions, θ and ϕ are considered to be constant over the time interval between successive solar pulses, but are assumed to vary from time interval to time interval. That is to say, θ and ϕ are both approximated by step functions which change values on the discrete set of discontinuities defined by the solar cell pulses. The solution is designed to evaluate these approximating functions step

by step. Rocket aspect will be determined when θ and ϕ are known; but if desired, the results may easily be expressed in terms of the more familiar azimuth and elevation angles. In this method of solution, there exist ambiguities which can normally be resolved without difficulty. We introduce constraints to force convergence to the correct choice of four possible solutions. To accomplish this, the quadrant of the angle θ and the direction of the spin of the missile must be known. The latter is usually predetermined, but can be measured if necessary, while the former is readily available through a proper interpretation of the trend in the amplitude of the magnetometer data. The necessary constraints follow:

1) $0 \leqslant \theta < \pi/2$ when the missile is nose-up,

2) $\pi/2 < \theta \leqslant \pi$ when the missile is nose-down,

3) $\dot{\psi} > 0$ for right-hand rotation,

4) $\dot{\psi} < 0$ for left-hand rotation,

where $\dot{\psi}$ is the spin rate of the rocket. If the results are desired in terms of the more familiar angles of azimuth and elevation, we note from Figure 6 that

$$\epsilon = \pi/2 - \theta \ , \tag{2}$$

$$\alpha = \begin{cases} \phi - \pi/2 \text{ when } \pi/2 \leqslant \phi \leqslant 2\pi \ , \\ \phi + 3\pi/2 \text{ when } 0 \leqslant \phi \leqslant \pi/2 \end{cases} \tag{3}$$

where α is defined as the azimuth measured counterclockwise from the X-axis and restricted to a range of from zero to 2π radians, while ϵ is the elevation angle with respect to the XY-plane.

In addition to our previous assumptions, we consider $\dot{\psi}$ to be constant between successive solar cell pulses so that

$$\dot{\psi} = \pm \frac{2\pi}{(t_f - t_o)} \ . \tag{4}$$

If ψ_i is the value of the Eulerian angle ψ at time t_i it follows that

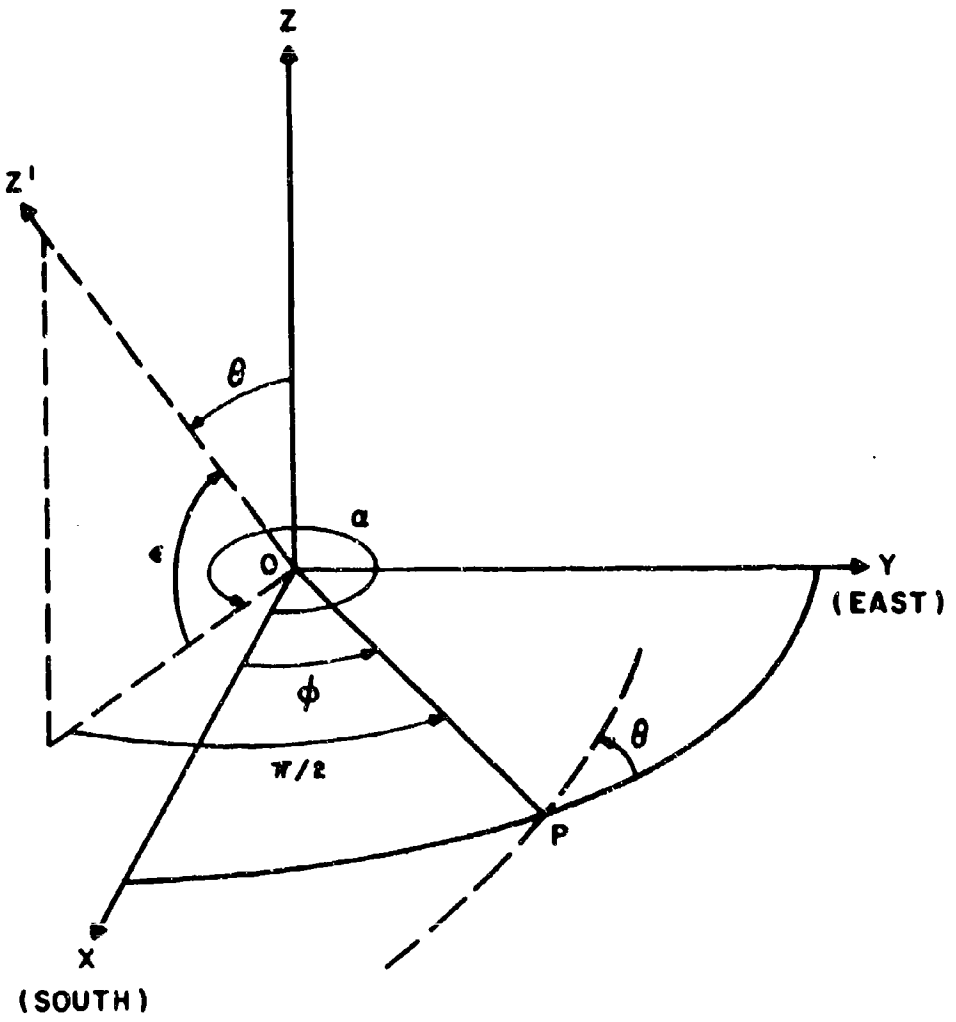

FIGURE 6 - ASPECT GEOMETRY

$$\psi_i = \psi_o + \dot{\psi}(t_i - t_o) , \qquad (5)$$

where ψ_o is the unknown value of ψ_i at time t_o. Shortly, it will be shown that ψ_o may be expressed as a function of θ and ϕ. Hence, the problem reduces to one of determining the step functions which approximate θ and ϕ.

In our development, we require notation for the direction cosines of several vectors in both coordinate systems. These will be denoted by (l, m, n) in the space coordinate system and (l', m', n') in the body system. In addition, the direction cosines will be further identified by the subscripts M, C, S, and H which correspond to the following vectors:

1) $\vec{M}$ is defined as a vector in the direction of the axis of the magnetometer.
2) $\vec{C}$ is a vector lying in the X'Y'-plane and directed from the origin of the coordinate system through the slit cut in the missile skin for the solar cell.
3) $\vec{S}$ is a vector from the origin of the coordinate system toward the sun.
4) $\vec{H}$ is the earth's magnetic field vector.

In the simplest approach to the problem, the vectors $\vec{S}$ and $\vec{H}$ may be considered constant in direction over the entire trajectory of the rocket. For greater accuracy, however, $\vec{S}$ can be varied with time and $\vec{H}$ with geometrical position provided that missile position is known as a function of time.

In the development of the solution, the direction cosines for the vectors $\vec{H}$ and $\vec{S}$ will be considered as known in the space reference frame. The direction of $\vec{H}$ may be determined either by direct measurement in the launching area or from series expansions using published spherical harmonic coefficients[9] while the direction cosines of $\vec{S}$ may be readily computed from ephemeris of the sun[10]. Hence, we regard (l_H, m_H, n_H) and (l_S, m_S, n_S) as known. The direction cosines of the vectors $\vec{M}$ and $\vec{C}$ are constant and known in the body coordinate system, but vary with time in

the space system. We may convert from the body to the space system by applying a transformation matrix which is the triple product of three separate rotations. Let this time variable matrix be detnoted by A_i. Then,

$$A_i = R_3(-\phi)R_1(-\theta)R_3(-\psi_i) \ , \tag{6}$$

where

$$R_3(-\phi) = \begin{pmatrix} \cos\phi & -\sin\phi & 0 \\ \sin\phi & \cos\phi & 0 \\ 0 & 0 & 1 \end{pmatrix} \ , \tag{7}$$

$$R_1(-\theta) = \begin{pmatrix} 1 & 0 & 0 \\ 0 & \cos\theta & -\sin\theta \\ 0 & \sin\theta & \cos\theta \end{pmatrix} \ , \tag{8}$$

$$R_3(-\psi_i) = \begin{pmatrix} \cos\psi_i & -\sin\psi_i & 0 \\ \sin\psi_i & \cos\psi_i & 0 \\ 0 & 0 & 1 \end{pmatrix} \ . \tag{9}$$

It follows that

$$\begin{pmatrix} l_{Mi} \\ m_{Mi} \\ n_{Mi} \end{pmatrix} = A_i \begin{pmatrix} l'_M \\ m'_M \\ n'_M \end{pmatrix} \ , \tag{10}$$

and

$$\begin{pmatrix} l_{Ci} \\ m_{Ci} \\ n_{Ci} \end{pmatrix} = A_i \begin{pmatrix} l'_C \\ m'_C \\ n'_C \end{pmatrix} \ . \tag{11}$$

The subscript i for the direction cosines in the space coordinate system simply indicates that these quantities vary with time, and therefore, refers to the particular time t_i.

By virtue of the definitions of the body coordinate system and the vectors $\vec{M}$ and $\vec{C}$ we have

$$\begin{pmatrix} l'_M \\ m'_M \\ n'_M \end{pmatrix} = \begin{pmatrix} 1 \\ 0 \\ 0 \end{pmatrix}, \tag{12}$$

and

$$\begin{pmatrix} l'_C \\ m'_C \\ n'_C \end{pmatrix} = \begin{pmatrix} \cos \omega \\ \sin \omega \\ 0 \end{pmatrix} , \tag{13}$$

where ω is defined as the angle between $\vec{C}$ and X'-axis. For our particular instrumentation system, $\vec{C}$ corresponds to the Y'-axis so that $\omega = \pi/2$ and

$$\begin{pmatrix} l'_C \\ m'_C \\ n'_C \end{pmatrix} = \begin{pmatrix} 0 \\ 1 \\ 0 \end{pmatrix} . \tag{14}$$

With this simplification, it immediately follows that the direction cosines (l_{Mi}, m_{Mi}, n_{Mi}) are given by the elements of the first column of the matrix A_i while (l_{Ci}, m_{Ci}, n_{Ci}) are obtained from the second column of the same matrix. Hence, we have

$$\begin{aligned} l_{Mi} &= \cos \phi \cos \psi_i - \sin \phi \cos \theta \sin \psi_i , \\ m_{Mi} &= \sin \phi \cos \psi_i + \cos \phi \cos \theta \sin \psi_i , \\ n_{Mi} &= \sin \theta \sin \psi_i , \end{aligned} \tag{15}$$

and

$$l_{Ci} = -(\cos\phi \sin\psi_i + \sin\phi \cos\theta \cos\psi_i) ,$$

$$m_{Ci} = \cos\phi \cos\theta \cos\psi_i - \sin\phi \sin\psi_i , \qquad (16)$$

$$m_{Ci} = \sin\theta \cos\psi_i .$$

It will now be shown that ψ_o, the value of ψ_i at time t_o, may be expressed in terms of the unknowns θ and ϕ. The vector $\vec{C}$ is in the direction of the Y'-axis. Referring to Figure 2, it is apparent that the vector $\vec{S}$ must lie in the Y'Z'-plane at t_o, a time at which a pulse is recorded for the solar cell. Moreover, the vector $\vec{M}$ is in the direction of the X'-axis so that $\vec{M}$ and $\vec{S}$ are orthogonal at t_o. The condition for orthogonality is

$$l_S l_{Mo} + m_S m_{Mo} + n_S n_{Mo} = 0 . \qquad (17)$$

Substituting from Equations (15) with $i = 0$ and solving for ψ_o yields

$$\psi_o = \tan^{-1}\left[\frac{l_S \cos\phi + m_S \sin\phi}{l_S \cos\theta \sin\phi - m_S \cos\theta \cos\phi - n_S \sin\theta}\right] . \qquad (18)$$

If we restrict ψ_o to lie between 0 and 2π radians, there are two possible solutions for ψ_o which satisfy Equation (18). However, we have an added condition which permits the complete resolution of this ambiguity. Since the solar cell is activated at time t_o, it is apparent that the sun is then contained in the solar cell acceptance beam, i.e., in the Y'Z'-plane and on the positive side of the X'Z'-plane (Figure 1). Hence, the angle between $\vec{S}$ and $\vec{C}$ must be equal to or less than $\pi/2$ radians so that

$$l_S l_{Co} + m_S m_{Co} + n_S n_{Co} \geq 0 . \qquad (19)$$

Combining Equations (16) with the Inequality (19) yields

$$\sin\psi_o(-l_S \cos\phi - m_S \sin\phi) + \cos\psi_o(-l_S \sin\phi \cos\theta + m_S \cos\phi \cos\theta + n_S \sin\theta) \geq 0. \qquad (20)$$

If we define N and D to be equal respectively to the numerator and denominator of the fraction in Equation (18), Inequality (20) may be written

$$-(N \sin \psi_o + D \cos \psi_o) \gtrless 0 \ . \tag{21}$$

Combining Equation (18) with Inequality (21) yields

$$-D \sec \psi_o \gtrless 0 \ , \tag{22}$$

$$-N \csc \psi_o \gtrless 0 \ . \tag{23}$$

Inequalities (22) and (23) uniquely determine in which quadrant ψ_o lies. The results are tabulated in Table I.

TABLE I

DETERMINATION OF THE RANGE FOR ψ_o IN RADIANS

Range of N	Range of D	Range of ψ_o
$N \leqslant 0$	$D < 0$	$0 \leqslant \psi_o < \pi/2$
$N < 0$	$0 \leqslant D$	$\pi/2 \leqslant \psi_o < \pi$
$0 \leqslant N$	$0 < D$	$\pi \leqslant \psi_o < 3\pi/2$
$0 < N$	$D \leqslant 0$	$3\pi/2 \leqslant \psi_o < 2\pi$

It is worth noting that ψ_o can still be expressed as a function of θ and ϕ when ω is not equal to $\pi/2$ radians. The procedure is completely analogous to the above derivation. The results will be presented without development. We have that

$$\tan \psi_o = \frac{N \sin \omega + D \cos \omega}{D \sin \omega - N \cos \omega} \ , \tag{24}$$

with the conditions that

$$-\sec \psi_o (D \sin \omega - N \cos \omega) \gtrless 0 \ , \tag{25}$$

$$-\csc \psi_o (D \cos \omega + N \sin \omega) \gtrless 0 \ . \tag{26}$$

As before, these permit a unique determination for ψ_o in the range from 0 to 2π radians.

We now consider the magnetometer measurements E_i from which we may derive an overdetermined system of condition equations. These measurements are proportional to the component of the geomagnetic field vector in the direction of the magnetometer axis, that is, the X'- axis of the body coordinate system. After normalization, the data constitute measurements of cos λ_i where λ_i is defined to be the angle between the vectors $\vec{M}$ and $\vec{H}$ at time t_i. We may then write the system of equations

$$l_H l_{Mi} + m_H m_{Mi} + n_H n_{Mi} = \cos \lambda_i \ , \tag{27}$$

for all values of i. In this system, the direction cosines (l_H, m_H, n_H) are considered known. Referring to Equations (5), (15) and (18) we note that (l_{Mi}, m_{Mi}, n_{Mi}) are functions of the two unknowns θ and ϕ. In practice, sufficient data are available be provide an overdetermined, but non-linear system of equations. A direct, least squares approach is, therefore, not possible. We resort to a computing procedure in which the unknowns are first approximated and then improved by a series of differential corrections. If second and higher order terms are omitted from the Taylor expansion about the point (θ, ϕ) which approximates the solution, the equations of condition may be written in matrix form as

$$J\Delta W = \Delta U. \tag{28}$$

where

$$\Delta W \equiv \begin{pmatrix} \Delta\theta \\ \Delta\phi \end{pmatrix} \ ,$$

$$J \equiv \left(\frac{\partial u_i}{\partial \theta} \ , \ \frac{\partial u_i}{\partial \phi} \right) \ ,$$

$$u_i \equiv \cos \lambda_i \ ,$$

$$\Delta U \equiv \left[(u_i)_{ob} - (u_i)_c \right] \ ,$$

for all values of i. The subscript ob refers to observed values while the subscript c indicates computed values derived from the approximate solution (θ, ϕ). Since the system is overdetermined, we obtain ΔW from the least squares solution

$$\Delta W = (J^*J)^{-1} J^* \Delta U , \tag{29}$$

where J^* is the transpose of the matrix J. Expressions for the evaluation of the elements of J may be found in the Appendix. Improved values for the unknowns are obtained from

$$W + \Delta W ,$$

where

$$W \equiv \begin{pmatrix} \theta \\ \phi \end{pmatrix} . \tag{30}$$

As a matter of convenience, no subscripts were introduced to indicate iteration. However, at this point in the computing procedure, the improved values of W are used as our approximate solution and the process is iterated until convergence is achieved. After convergence, the azimuth and elevation angles, which completely describe rocket aspect, may be computed from Equations (2) and (3).

Frequently, in differential correction computations, it is difficult if not impossible to initially approximate the unknowns with sufficient accuracy to assure convergence to the correct result. It is notable, however, that the method presented herein has been found to converge for any initial approximations of the unknown angles that lie within the permissible ranges of 0 to 2π radians for ϕ, and either 0 to $\pi/2$ radians or $\pi/2$ to π radians for θ. Tabulated in Table II are the results of a series of computations for a particular set of actual field data. Initial approximations for θ and ϕ have been varied over the entire ranges of these two angles. In each instance, the computation converged to the same result. The number of iterations required for convergence has also been tabulated. As expected, the better approximations require fewer iterations and therefore, less computing time; but even poor starting values eventually lead to correct results. In practice, when aspect is

computed for a sequence of points spaced at short time intervals, the number of iterations, and hence computing time, is held to a minimum by using the results for previous points to arrive at good initial approximations for the unknown angles.

TABLE II

TEST OF COMPUTING PROCEDURE FOR CONVERGENCE

Computing Input		Computing Output		Number of
α	ϵ	α	ϵ	Iterations
0°	89°	18.922°	86.983°	5
90°	89°	18.922°	86.983°	14
180°	89°	18.922°	86.983°	17
270°	89°	18.922°	86.983°	9
0°	45°	18.922°	86.983°	5
90°	45°	18.922°	86.983°	8
180°	45°	18.922°	86.983°	8
270°	45°	18.922°	86.983°	9
0°	1°	18.922°	86.983°	8
90°	1°	18.922°	86.983°	13
180°	1°	18.922°	86.983°	13
270°	1°	18.922°	86.983°	28

DISCUSSION OF SYSTEM ERROR SOURCES

All magnetometer systems suffer from one basic shortcoming; namely, that elimination of magnetic interference is tedious. However, the payloads in which this system has been flown were designed primarily for measurement of the geomagnetic field and consequently the payload components were chosen to have small magnetic moments. The static magnetic field perturbation (due to permanent and induced magnetism) at the aspect magnetometer sensor was measured for a range of payload orientation and found to be less than 0.1 percent of the earth's magnetic field.

Disturbances due to electrical currents were of similar magnitude, except during the interval from 30 to 60 seconds, when a known disturbance, due to a proton precession magnetometer, took place during 50 percent of the measurements. These measurements have not been corrected, and consequently the data scatter during this time is large.

Another source of magnetic disturbance, often neglected in the use of aspect magnetometers, is the attenuation and rotation of the geomagnetic field within the payload due to currents induced by the field in a spinning, conducting rocket structure. The structure of the nose cones under discussion was fiberglass and there was no appreciable amount of metal near the magnetometers, so that induced currents were negligible.

Alignment of the magnetic and optical axes is easily handled by standard machine shop practice to an angular accuracy greatly exceeding that necessary for this application. The alignment of the aspect magnetometer axis with the mechanical structure of the sensor is within 1/4 to 1/2 degree, so that mechanical alignment assures magnetic alignment.

The systematic error in the magnetometer measurement is estimated to be less than one percent, corresponding to an error of 1/2 degree in elevation and 10 degrees in azimuth, or a pointing error of less than 2 degrees during the vacuum portion of flight. This is the estimated maximum systematic error from this source and the actual value is probably considerably less.

Rocket aspect errors resulting from errors in the solar cell time pulse have been estimated and the results plotted in Figure 7. A time error equivalent to one percent of the rocket spin period was assumed and error propagation into missile aspect was computed with data that were otherwise free of error. The results are presented as a function of rocket attitude with the azimuth angle plotted as the polar angle and the elevation angle as the radius vector. Contour lines for errors of 1, 3, and 5 degrees have been drawn. The assumed time error of one percent of the spin period is larger than anticipated for the measuring system; yet, the resulting aspect error at higher elevation angles is not

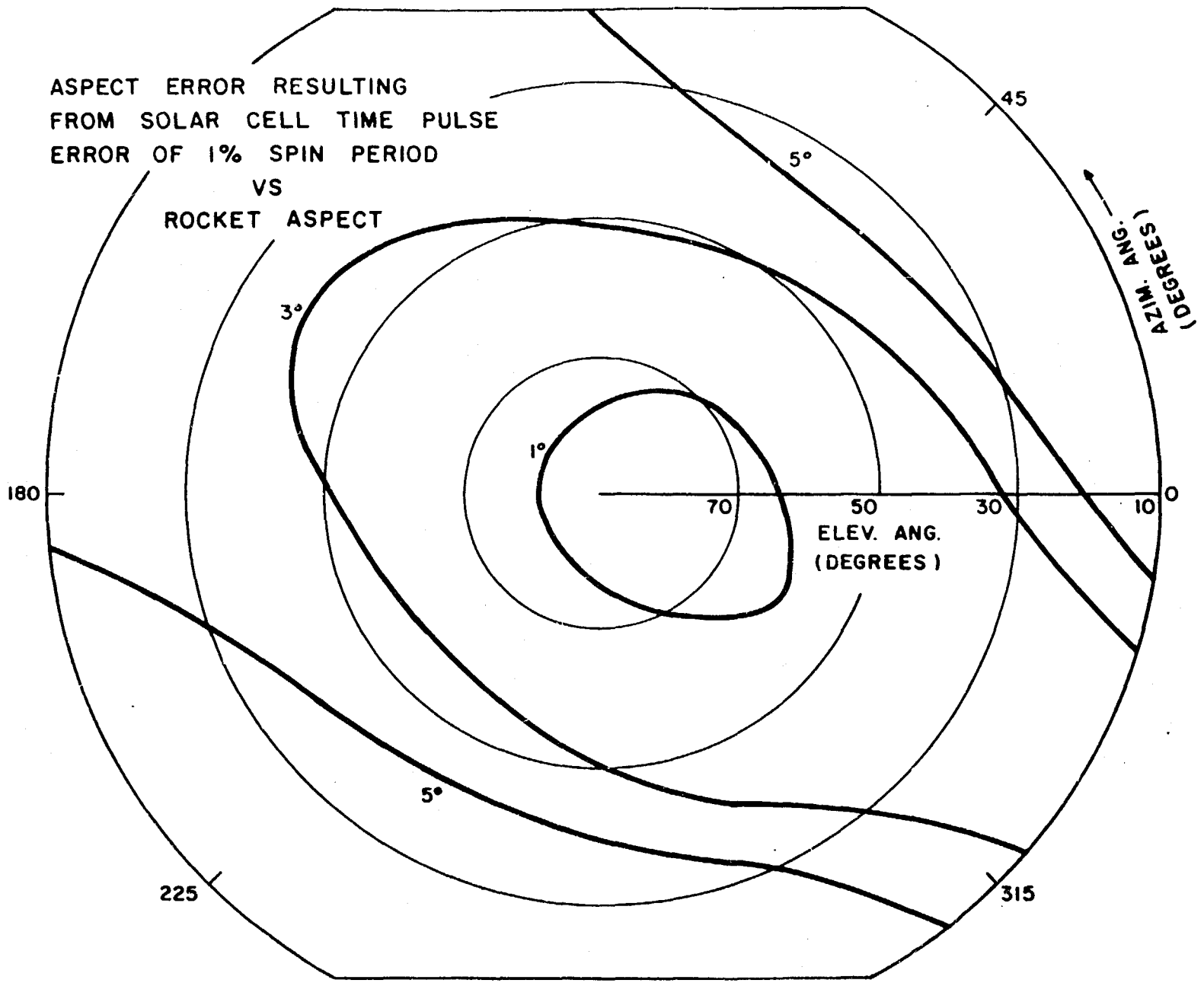
ASPECT ERROR RESULTING
FROM SOLAR CELL TIME PULSE
ERROR OF 1% SPIN PERIOD
VS
ROCKET ASPECT
45
5°
3°
1°
180
0
70
50
30
10
ELEV. ANG.
(DEGREES)
AZIM. ANG.
(DEGREES)
5°
225
315

FIGURE 7

excessive. It is estimated that time errors in the solar cell pulse will normally not exceed 0.5 percent of the spin period. However, since the aspect error varies almost linearly with the time error, Figure 8 may still be used to estimate the effect of the smaller time errors by decreasing the system error in proportion to the decrease in the time error. The orientation of the contour lines in Figure 8 is closely related to the direction of the vectors $\vec{S}$ and $\vec{H}$. Both vectors were assumed to be identical with those employed in the reduction of the measured data which are presented in the following section. It is of interest that the minimum propagation of error occurs in the direction of the sun which was approximately 30 degrees west of south.

An independent knowledge of both magnitude and direction of the earth's magnetic field is necessary when only a single aspect magnetometer is employed. Both magnitude and direction are well known at Fort Churchill. Table III is a list of the measured and calculated values of total field, inclination, and declination. Only a severe magnetic storm would cause errors greater than those already inherent in the system. In the data reduction, an eccentric dipole model based on rocket measurements[11] was used to calculate the magnitude of the field. Declination and inclination were considered constant throughout the rocket trajectory, since the variation of these quantities is indicated to be less than 1/2 degree from the Jensen and Cain model[9].

COMPUTATIONAL RESULTS

The computing method, which has been presented, was applied to aspect data recorded for Nike-Apache Rocket No. 14.36, launched at Fort Churchill, Canada, on 7 October 1963. Reductions were obtained for most of the usable data and cover three sections of the flight. The first period, which extends from 5 to 37.5 seconds after launch, is of particular interest since it is possible to compare the results from the aspect system with missile attitudes derived from DOVAP[12] (DOppler Velocity And Position) reductions. The aspect results for the second period

TABLE III

TOTAL SCALAR FIELD

Measured at Ground (Proton Magnetometer)	61,120 γ*
Extrapolated to Ground from Rocket Measurement [11]	61,240 γ
Jensen and Cain Analysis[9]	61,320 γ

INCLINATION

Measured at Ground (Dip Circle)	83° 32' ± 5'
Jensen and Cain	83° 33'

DECLINATION

Measured at Ground (Variometer)	(East of North)	2° 35' ± 20'
Jensen and Cain	(East of North)	2° 26'

*10^5 γ = 1 gauss

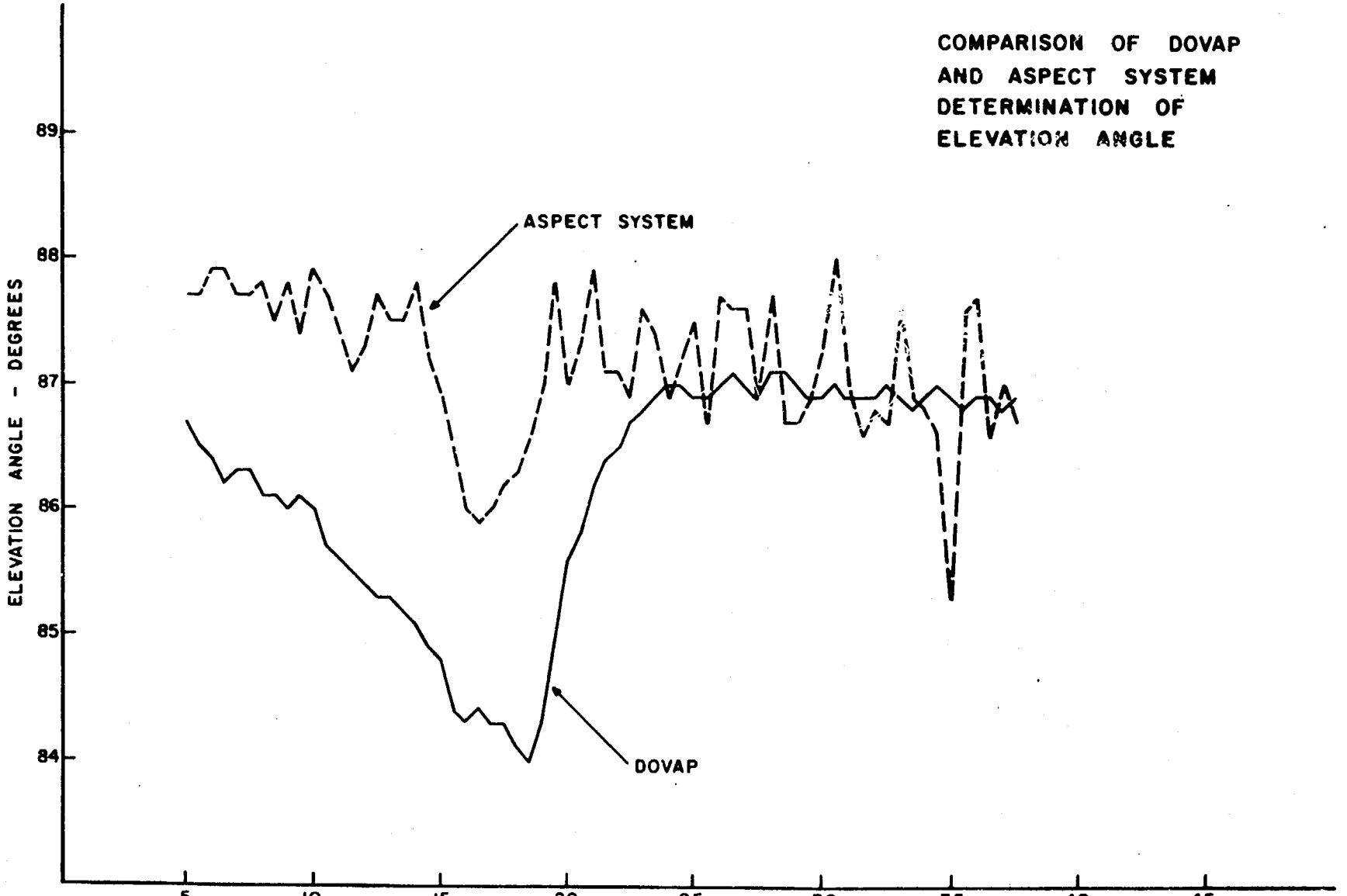
COMPARISON OF DOVAP
AND ASPECT SYSTEM
DETERMINATION OF
ELEVATION ANGLE
ASPECT SYSTEM
DOVAP
ELEVATION ANGLE - DEGREES
89
88
87
86
85
84
5
10
15
20
25
30
35
40
45
TIME - SECONDS

FIGURE 8

from 265 to 342.5 seconds indicate that the rocket slowly nosed over as it re-entered the effective atmosphere. Finally, after 346 seconds, the missile underwent a period of coning which was continuously damped as the missile gradually approached vertical flight with the nose downward at 375 seconds.

The comparison of the aspect results with the DOVAP reductions yielded better agreement than anticipated. The DOVAP system normally provides highly accurate determinations of rocket position and velocity as a function of time. However, missile spin introduces accumulative phase errors into the DOVAP data[13]. Ordinarily, these errors may be measured and the raw data rather accurately corrected. Occasionally, as a result of poor antenna patterns, the spin corrections are of doubtful quality. In the case under consideration, the spin errors were particularly difficult to detect and correct. Therefore, the DOVAP reductions very likely contain rather serious spin errors. These enter the results primarily as systematic rather than random errors since a portion of the spin correcting procedure consists of smoothing data which have been corrected for the errors introduced by spin.

DOVAP reductions normally provide a relatively smooth trajectory which may be differentiated numerically to obtain rather accurate velocity components. If we assume that the velocity vector lies along the symmetry axis of the missile while the latter is still in the effective atmosphere, we may use the DOVAP velocity components to compute rocket attitude as a function of time. This has been done for the period from 5 to 37.5 seconds and the results have been plotted in Figures 8 and 9 together with the reductions obtained from the aspect system. Both sets of data show the elevation angle of the rocket to initially decrease and later increase. The latter event coincides with the initiation of second-stage burning. While agreement between the two systems appears to be poor for the azimuth over the early portion of the trajectory, it should be noted that the azimuth is not particularly significant when the elevation angle approximates $\pi/2$ radians. A more significant comparison between the two sets of data may be obtained from Figure 10 which

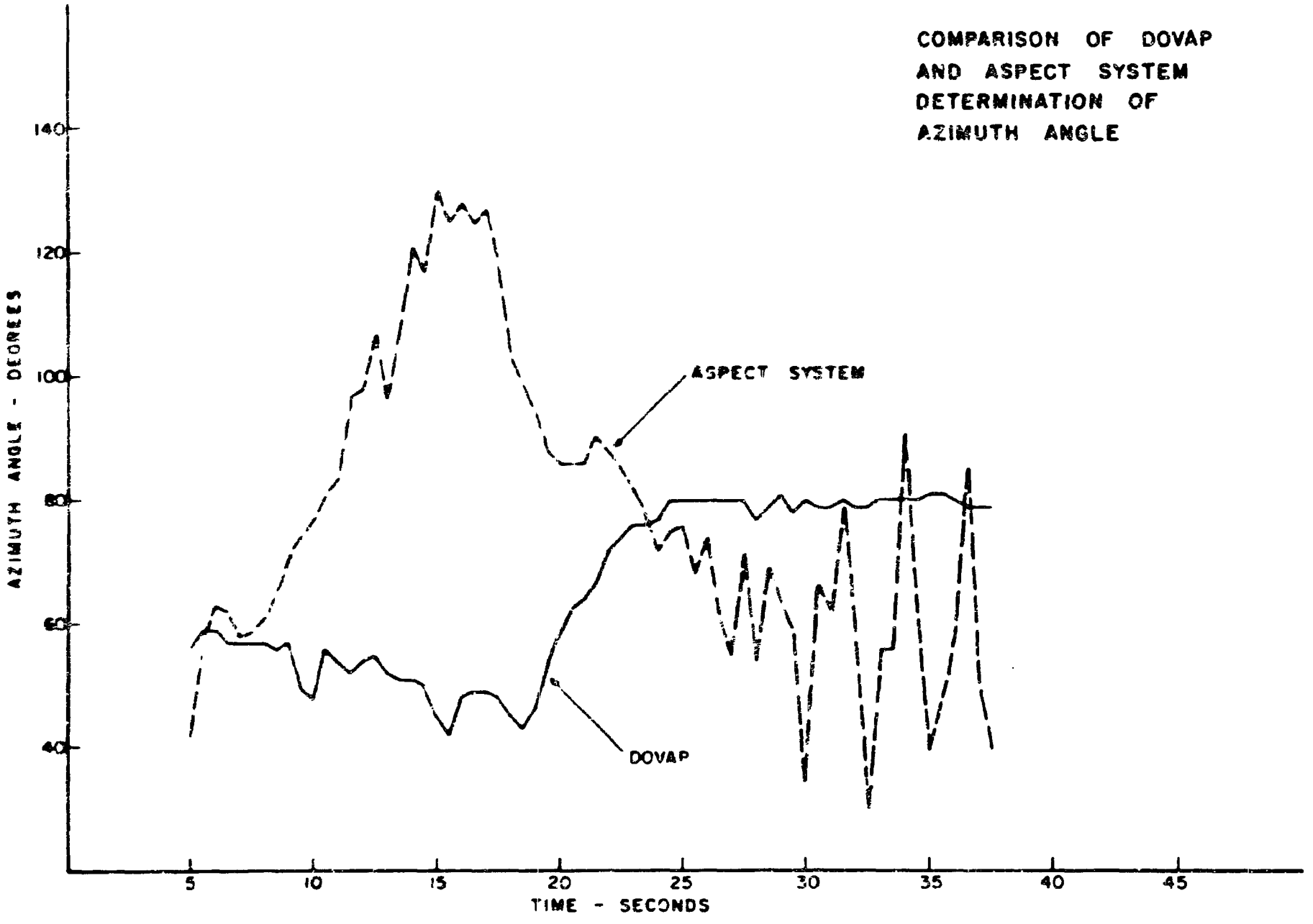
COMPARISON OF DOVAP AND ASPECT SYSTEM DETERMINATION OF AZIMUTH ANGLE
AZIMUTH ANGLE - DEGREES
140
120
100
80
60
40
ASPECT SYSTEM
DOVAP
5
10
15
20
25
30
35
40
45
TIME - SECONDS

FIGURE 9

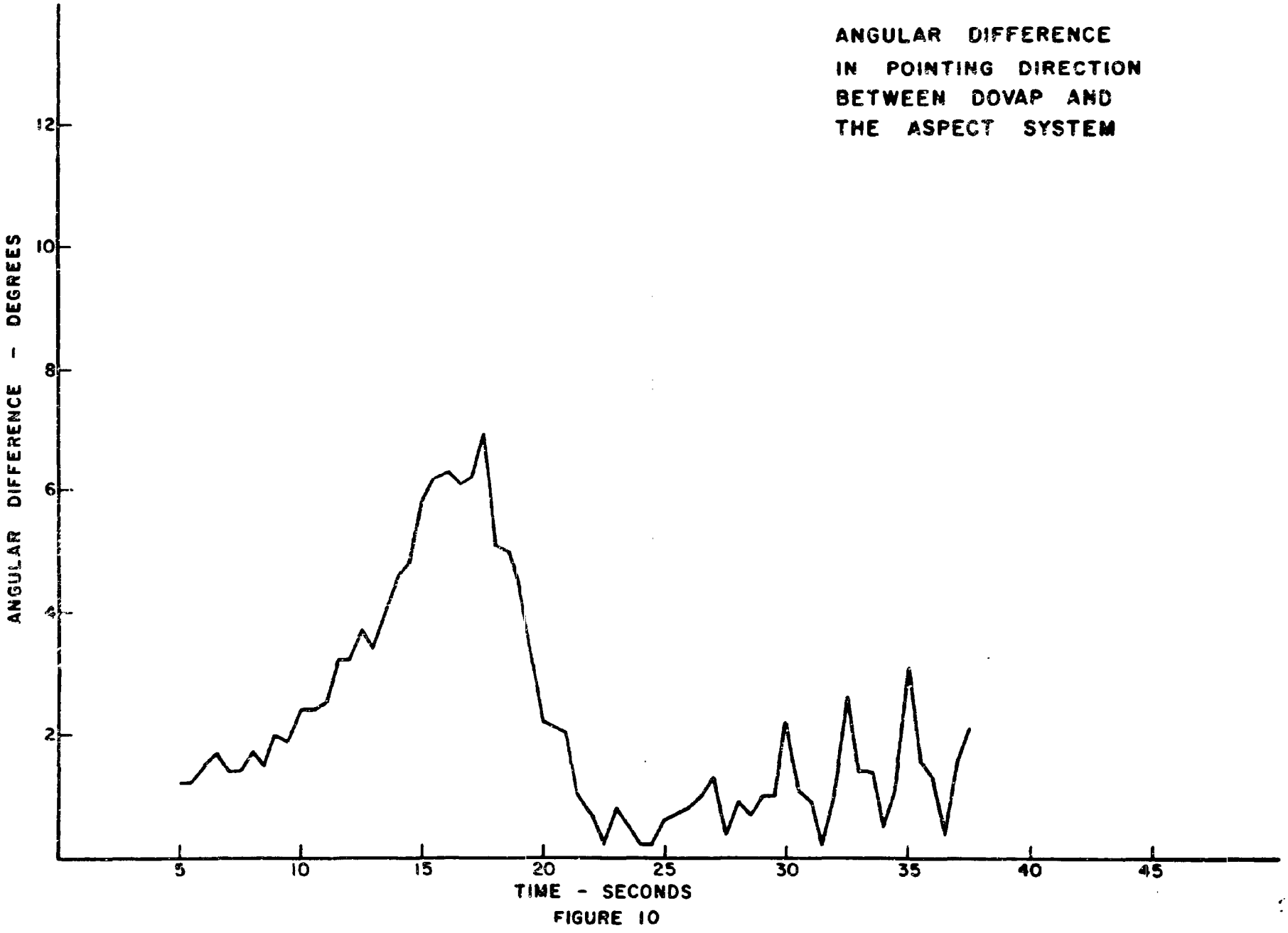
ANGULAR DIFFERENCE
IN POINTING DIRECTION
BETWEEN DOVAP AND
THE ASPECT SYSTEM
ANGULAR DIFFERENCE - DEGREES
12
10
8
6
4
2
5
10
15
20
25
30
35
40
45
TIME - SECONDS

FIGURE 10

presents a plot of the angle between the two determinations of the rocket aspect vector as a function of time. Although this angle reaches a maximum of about 7 degrees early in flight, the two systems agree, on the average, to within 1.5 degrees between 20 and 37.5 seconds. This is remarkable since the aspect system itself was designed for approximately 1 degree accuracy, and it is estimated that the errors in the DOVAP system are of this order of magnitude. The extreme roughness in the reductions for the aspect system in the period from 30 to 37.5 seconds was expected. It resulted from interference by the polarization field of a proton precession magnetometer which was also carried on board the rocket Estimates of probable error obtained from the least squares solution for the aspect system are on the average about 0.3 degree in elevation angle and 6.5 degrees in azimuth over the entire interval from 5 to 37.5 seconds. A polar plot of the two determinations of rocket aspect for the initial reduction period is presented in Figure 11. Azimuth has been plotted as the polar angle and elevation as the radius vector. The numbered positions are at five second intervals. In comparing the reduced data for these two systems, it should be recalled that while the DOVAP results have small random errors, they undoubtedly contain rather serious systematic errors as a result of missile spin.

The next period of interest runs from 265 to 342.5 seconds. Plots of both the elevation and azimuth angles are presented as a function of time in Figure 12. These graphs clearly indicate that the rocket was precessing at a rate of approximately 6 degrees per second before its re-entry into the effective atmosphere at approximately 330 seconds. Throughout this period of precessing motion, the elevation angle varied between extremes of 61 degrees and 86 degrees while the azimuth ranged from 172 degrees to 269 degrees. The plots in Figure 12 show that the rocket, following re-entry, began to nose over as the elevation angle decreased from 85 degrees to 45 degrees in the period from 330 to 342.5 seconds. After a short break of about four seconds in the recorded data of the aspect system, the reductions show that the missile nosed over and entered a stage of coning which was gradually damped during the

COMPARISON OF DOVAP AND ASPECT SYSTEM DETERMINATION OF ROCKET ATTITUDE

POINT NO.	FLIGHT TIME
1	5 SEC.
2	10
3	15
4	20
5	25
6	30
7	35

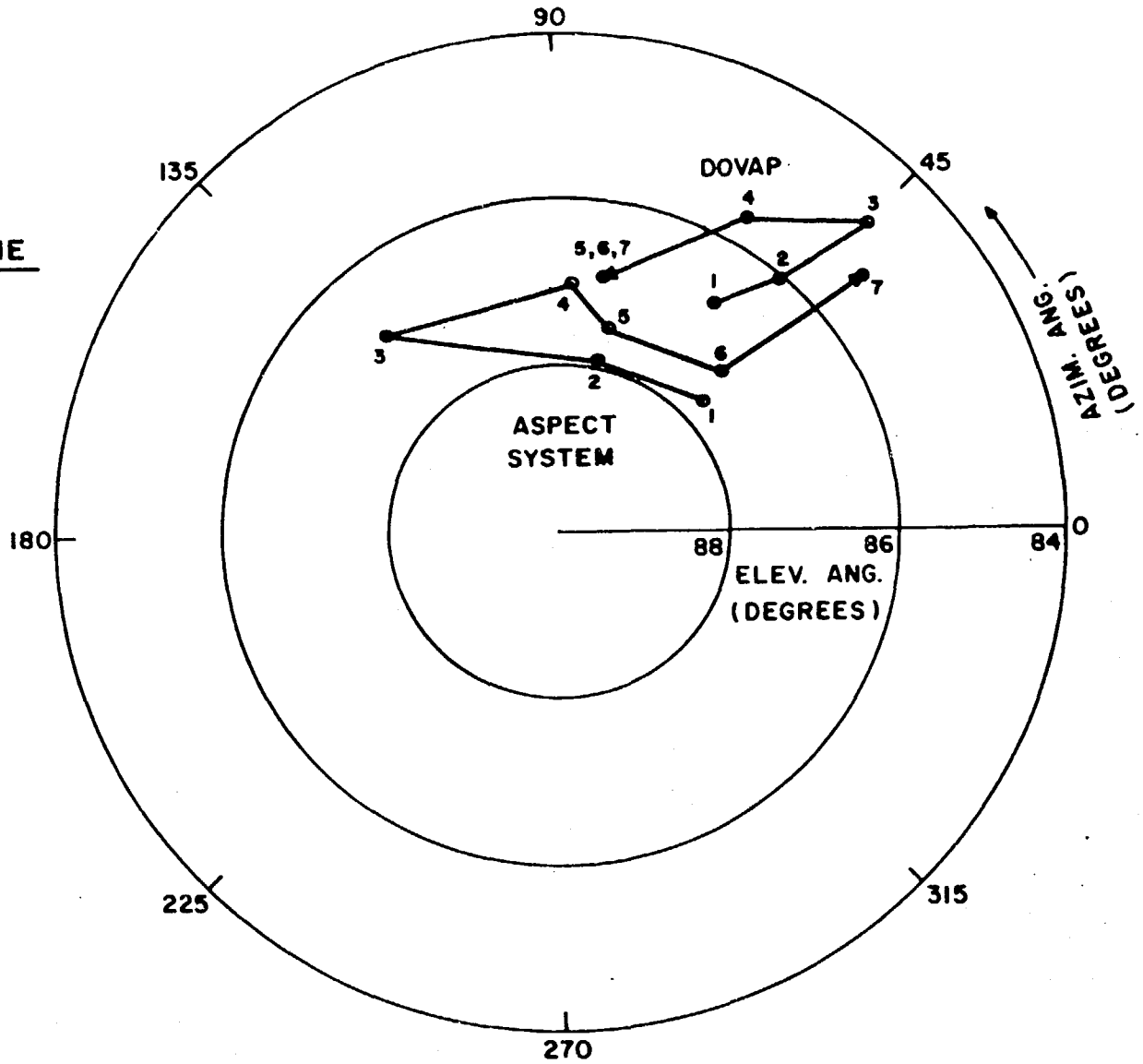

FIGURE 11

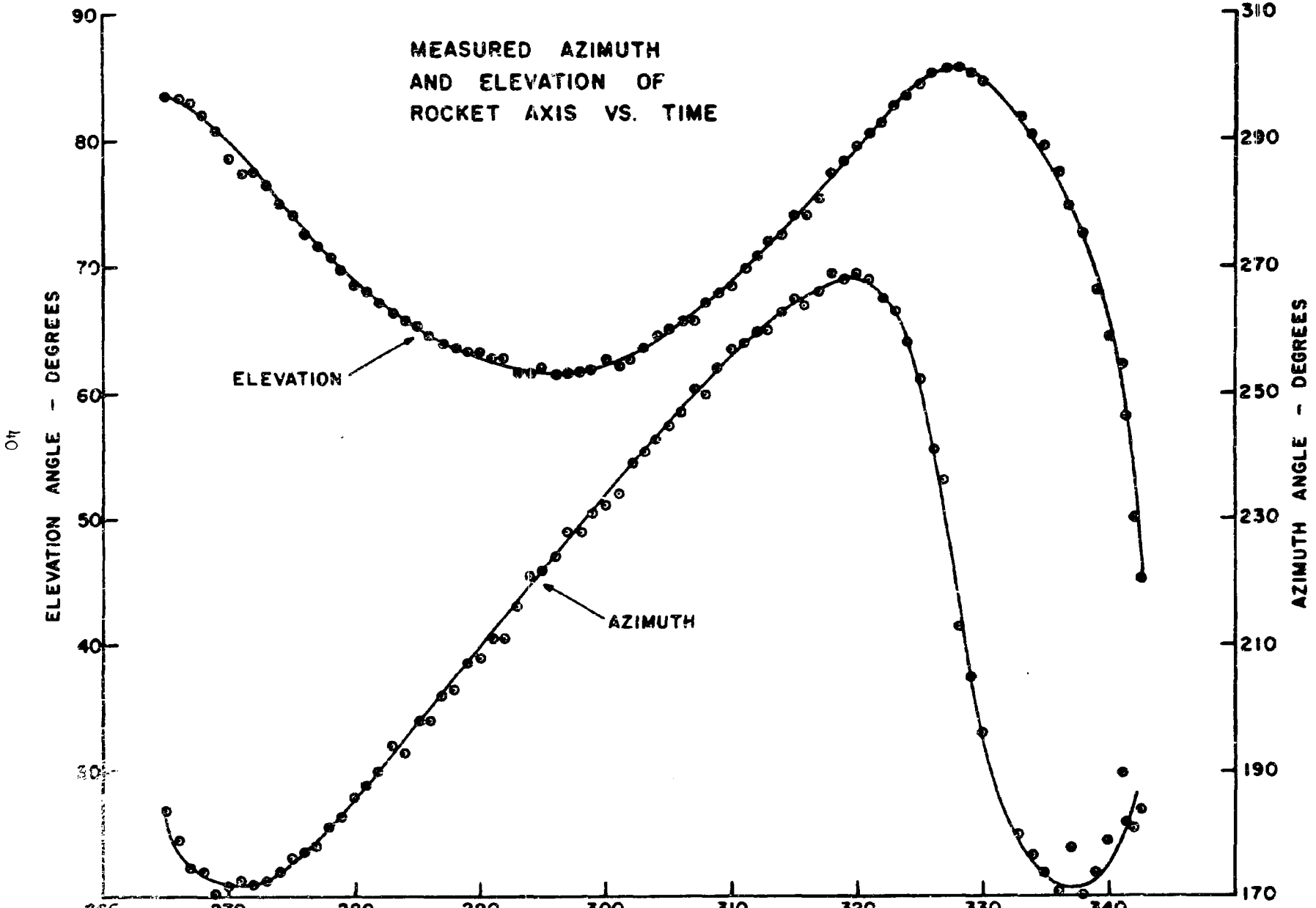
MEASURED AZIMUTH
AND ELEVATION OF
ROCKET AXIS VS. TIME
ELEVATION
AZIMUTH
ELEVATION ANGLE - DEGREES
AZIMUTH ANGLE - DEGREES
TIME - SECONDS
90
80
70
60
50
40
30
310
290
270
250
230
210
190
170
260
270
280
290
300
310
320
330
340

FIGURE 12

remaining period of observation. The aspect measurements may be easily interpreted from the series of polar plots presented in Figures 13A through 14A. As before, azimuth is plotted as the polar angle while the negative elevation angle is plotted as the radius vector. The terminal point of each graph is also the initial point of the following figure. Flight time has been indicated periodically. To aid in the interpretation of the reduced data, continuous curves have been drawn through the plotted points. With the aid of these polar plots, curves showing the variation of the azimuth and elevation angles with time were derived and are presented in Figures 15 and 16.

CONCLUSION

The aspect measuring system, described in this report, has been found to provide a practical and inexpensive approach for the accurate determination of the attitude of spinning rockets. While the system has certainly not been precisely evaluated for accuracy, the comparison of the aspect reductions with DOVAP results gave better agreement than expected. Recalling that the DOVAP spin-error corrections had a low confidence level for this particular rocket, it is considered likely that the errors in the results for the aspect system were smaller than those in the DOVAP determinations. On the basis of these initial results, the attitude sensor is estimated to have provided an over-all accuracy of one to two degrees in the determination of rocket aspect. Moreover, it appears likely that the sensor has a potential accuracy of better than one degree.

The method of solution has been shown to be practical. It readily lends itself to rapid computation on a large scale digital computer. On the average, one determination of missile aspect required 3 to 4 iterations and was computed at the rate of 0.16 seconds per iteration on the BRLESC computer so that a single solution for rocket aspect required approximately 0.6 seconds of computing time. There are no ambiguities in the results if the direction of spin and the sign of the elevation angle are known. The latter may be determined from the magnetometer

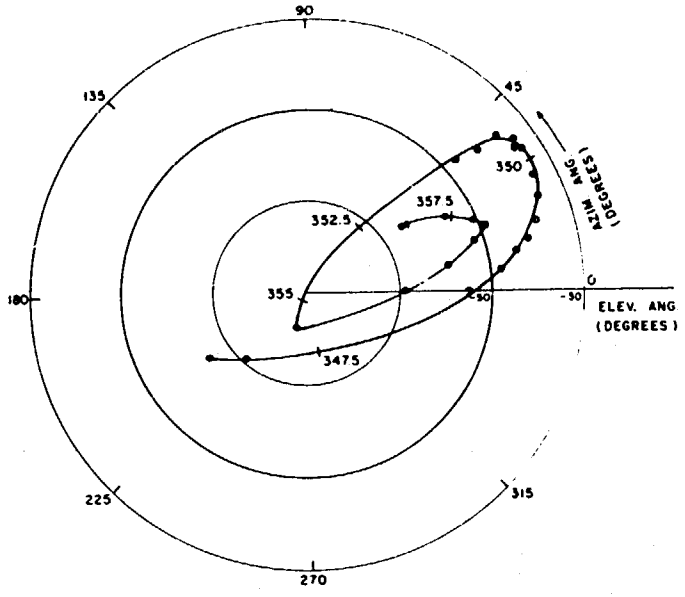

13A

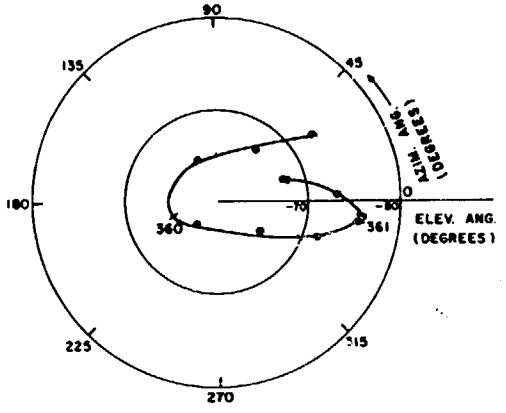

13B

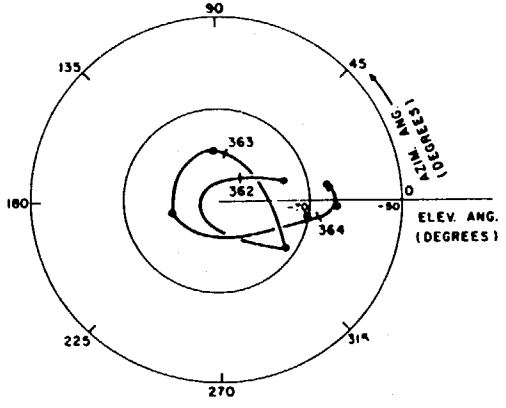

13C

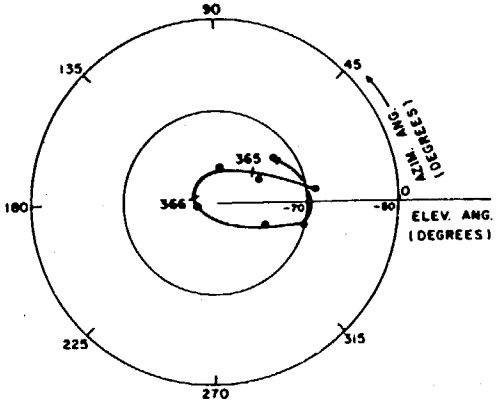

13D

FIGURE 13 – ASPECT SYSTEM MEASUREMENTS

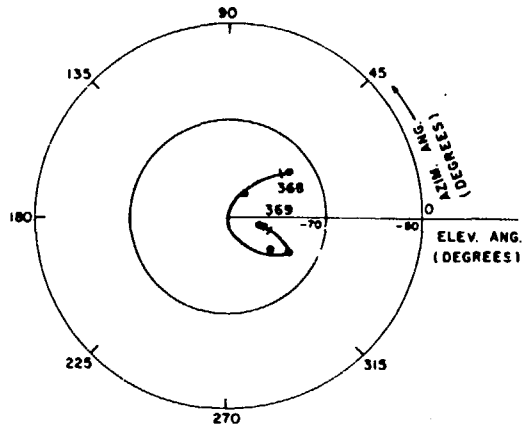

14A

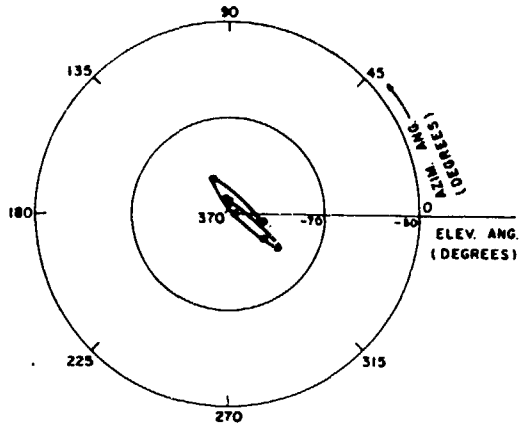

14B

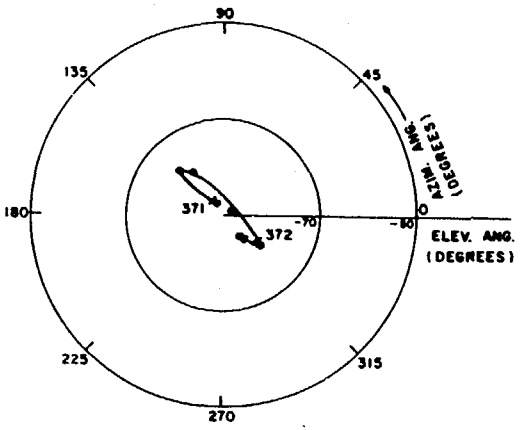

14C

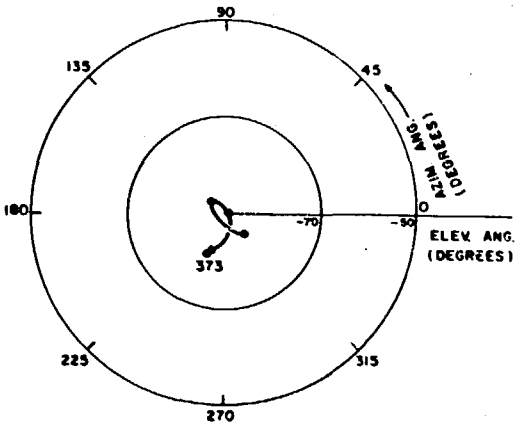

14D

FIGURE 14—ASPECT SYSTEM MEASUREMENTS

MEASURED AZIMUTH OF
ROCKET AXIS VS. TIME

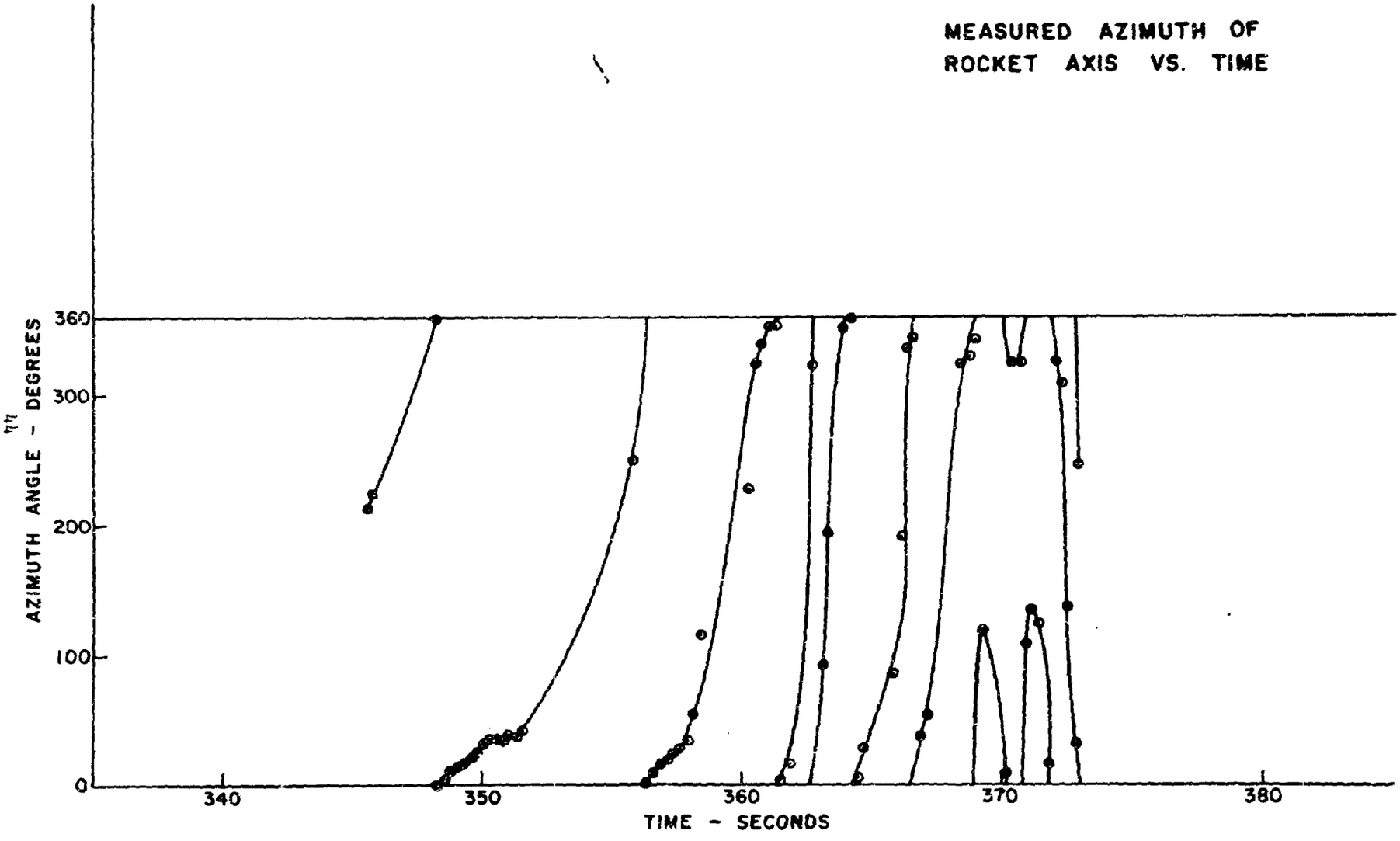

FIGURE 15

MEASURED ELEVATION OF
ROCKET AXIS VS. TIME

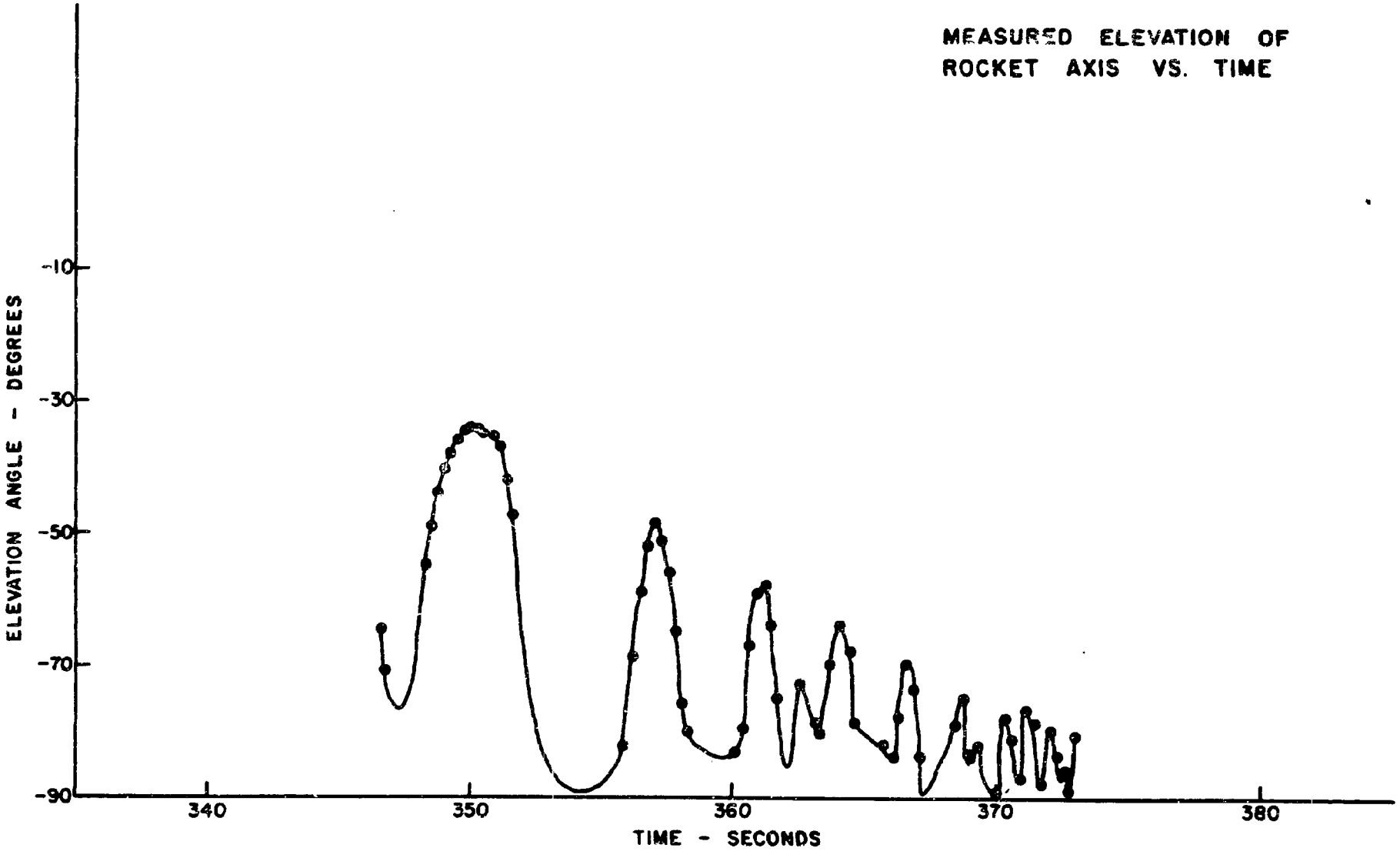

FIGURE 16

record while the direction of spin is usually a known characteristic of the rocket. With ambiguities resolved, convergence to a unique solution in reasonable computing time is assured.

JOSEPH M. CONLEY R. B. PATTON, JR.

REFERENCES

1. Ito, M. Analysis of the Output of Rocket-Borne Magnetometers. Can. J. Phys., 41, 1252-1262, 1963.

2. Marks, Spence T. and Conley, Joseph M. Instrumentation, Flight Summaries and Aspect Data of Nike-Cajun Rockets OB 6.04, OB 6.06 and OB 6.15. Ballistic Research Laboratories Memorandum Report No. 1214, 1959.

3. Israel, G., Kiveliovitch, M., and Vassey, A. Compt. rend, 253, 2317, 1961.

4. Albus, James. A Digital Solar Aspect Sensor. National Aeronautics and Space Administration T. N. D-1602, 1961.

5. Conley, Joseph M. and Prosser, James F. A Solar Aspect Device for Sounding Rockets. Ballistic Research Laboratories Technical Note No. 1464, 1962.

6. Kupperian, James E. and Kreplin, Robert W. Optical Aspect System for Rockets. Rev. Sci. Inst., 28, 14-19, 1957.

7. Gross, M. J. and Heddle, D. W. O. The Angular Motion of a Freely Falling Rocket. Proc. Roy. Soc. A, 279, 523-533, 1964.

8. Goldstein, Herbert. Classical Mechanics. Cambridge, Mass., Addison-Wesley Publishing Co., Inc., 1953.

9. Jensen, D. C. and Cain, J. C. An Interim Geomagnetic Field (Abstract). J. Geophys. Res., 67, 3568, 1962.

10. The American Ephemeris and Nautical Almanac. Washington, D. C., U.S. Government Printing Office.

11. Conley, Joseph M. Earth's Main Magnetic Field to 152 Kilometers Above Fort Churchill. J. Geophys. Res., 65, 1074, 1960.

12. deBey, A. L. G., and Hoffleit, E. Dorrit. DOVAP----Instrumentation and Analysis of Operational Results. Ballistic Research Laboratories Report No. 677, 1948.

13. Patton, R. B. Jr. An Analysis of Spin Errors in the DOVAP System from the Record of Bumper Round No. 5. Ballistic Research Laboratories Memorandum Report No. 504, 1950.

APPENDIX

Evaluation of the Elements of J

The Jacobian matrix J has been defined as

$$J \equiv \left(\frac{\partial u_i}{\partial \theta} , \frac{\partial u_i}{\partial \phi} \right) ,$$

for all values of i. We also have the relation

$$l_H \, l_{Mi} + m_H \, m_{Mi} + n_H \, n_{Mi} = u_i \quad .$$

Using this expression with Equations (5), (15), and (18), we obtain the following partial derivatives which may be used to evaluate the elements of J:

$$\frac{\partial u_i}{\partial \theta} = l_H \frac{\partial l_{Mi}}{\partial \theta} + m_H \frac{\partial m_{Mi}}{\partial \theta} + n_H \frac{\partial n_{Mi}}{\partial \theta} \quad ,$$

$$\frac{\partial u_i}{\partial \phi} = l_H \frac{\partial l_{Mi}}{\partial \phi} + m_H \frac{\partial m_{Mi}}{\partial \phi} + m_H \frac{\partial n_{Mi}}{\partial \phi} \, ,$$

$$\frac{\partial l_{Mi}}{\partial \theta} = \sin\theta \sin\phi \sin \psi_i - (\sin \psi_i \cos\phi + \cos\theta \sin\phi \cos \psi_i) \frac{\partial \psi i}{\partial \theta} \quad ,$$

$$\frac{\partial m_{Mi}}{\partial \theta} = -\sin\theta \cos\phi \sin \psi_i + (\cos\theta \cos\phi \cos \psi_i - \sin\phi \sin \psi_i) \frac{\partial \psi i}{\partial \theta} \quad ,$$

$$\frac{\partial n_{Mi}}{\partial \theta} = \cos\theta \sin \psi_i + \sin\theta \cos \psi_i \frac{\partial \psi i}{\partial \theta} \quad ,$$

$$\frac{\partial l_{Mi}}{\partial \phi} = -(\cos \psi_i \sin\phi + \cos\theta \cos\phi \sin \psi_i) - (\sin \psi_i \cos\phi + \cos\theta \sin\phi \cos \psi_i) \frac{\partial \psi_i}{\partial \phi} ,$$

$$\frac{\partial m_{Mi}}{\partial \phi} = (\cos \psi_i \cos\phi - \cos\theta \sin\phi \sin \psi_i) + (\cos\theta \cos\phi \cos \psi_i - \sin \psi_i \sin \phi) \frac{\partial \psi_i}{\partial \phi} ,$$

$$\frac{\partial n_{Mi}}{\partial \phi} = (\sin\theta \cos \psi_i) \frac{\partial \psi_i}{\partial \phi} ,$$

$$\frac{\partial \psi_i}{\partial \theta} = \frac{\sin^2 \psi_o}{N} (l_S \sin\theta \sin\phi - m_S \sin\theta \cos\phi + n_S \cos\theta) ,$$

$$\frac{\partial \psi_i}{\partial \phi} = \frac{\sin \psi_o}{N} (m_S l_{Mo} - l_S m_{Mo}).$$